

Article

Evolution of the Microstructure and Mechanical Properties of a Biomedical Ti-20Zr-40Ta Alloy during Aging Treatment

Xueqing Wu ¹, Kun Yang ², Jun Cheng ³ and Jianguo Lin ^{2,*}

¹ School of Physics and Electronic Science, Guizhou Normal University, Guiyang 550001, China; xueqingwu1@sohu.com

² School of Materials Science and Engineering, Xiangtan University, Xiangtan 411105, China

³ Northwest Institute for Nonferrous Metal Research, Shaanxi Key Laboratory of Biomedical Metal Materials, Xi'an 710016, China

* Correspondence: lin_j_g@xtu.edu.cn

Abstract: The research focus in the field of medical titanium alloys has recently shifted towards the development of low-modulus and high-strength titanium alloys. In this study, the influence of aging temperature on the microstructure and mechanical properties of a β -type Ti-20Zr-40Ta alloy (TZT) was investigated. It was found that the recovery and the recrystallization occurred in the as-rolled alloy depended on the aging temperature. The periodically distributed Ta-lean phase (β_1) and Ta-rich phase (β_2) were produced by the spinodal decomposition in all the samples aged at different temperatures. The spinodal decomposition significantly influenced the mechanical properties and deformation mechanisms of the TZT alloy. Upon aging at 650 °C and 750 °C, the as-rolled alloy exhibited a double-yield phenomenon during tensile testing, indicating a stress-induced martensitic transformation; however, its ductility was limited due to the presence of ω phases. Conversely, aging at 850 °C resulted in an alloy with high strength and good ductility, which was potentially attributed to the enhanced strength resulting from modulated structures introduced with spinodal decomposition.

Keywords: Ti-20Zr-40Ta alloy; spinodal decomposition; microstructure; mechanical property



Citation: Wu, X.; Yang, K.; Cheng, J.;

Lin, J. Evolution of the

Microstructure and Mechanical

Properties of a Biomedical

Ti-20Zr-40Ta Alloy during Aging

Treatment. *Coatings* **2024**, *14*, 590.

[https://doi.org/10.3390/](https://doi.org/10.3390/coatings14050590)

[coatings14050590](https://doi.org/10.3390/coatings14050590)

Academic Editor: Seunghan Oh

Received: 18 April 2024

Revised: 30 April 2024

Accepted: 7 May 2024

Published: 9 May 2024



Copyright: © 2024 by the authors.

Licensee MDPI, Basel, Switzerland.

This article is an open access article

distributed under the terms and

conditions of the Creative Commons

Attribution (CC BY) license ([https://](https://creativecommons.org/licenses/by/4.0/)

[creativecommons.org/licenses/by/](https://creativecommons.org/licenses/by/4.0/)

[4.0/](https://creativecommons.org/licenses/by/4.0/)).

1. Introduction

The materials utilized for bone implantation typically necessitate high strength and a low elastic modulus. Conventional titanium alloys, like Ti-6Al-4V, possess a lower elastic modulus compared to other metallic materials [1]; however, their elastic modulus still exceeds that of human bone (4–30 GPa) [2]. This may lead to the development of a phenomenon known as the “stress shielding effect” when implanted in the human body, which could potentially contribute to an early deterioration of the implants [3,4]. Incorporation of non-toxic β stabilizing elements (such as Ta, Nb, Mo, etc.) has led to the development of a range of metastable titanium alloys with a β -type structure in recent years. These alloys exhibit significantly reduced elastic moduli comparable to those of human bones [5–8]. For instance, the elastic modulus range for the β -type Ti-29Nb-13Ta-4.6Zr alloy is approximately 50–55 GPa [9], while the Ti-24Nb-4Zr-8Sn alloy (Ti2448) demonstrates an even lower elastic modulus at around 40 GPa [10].

High strength is a crucial requirement for bone implant materials. However, the alloying or microstructure regulation of Ti alloys typically leads to a decrease in their elastic modulus and subsequently compromises their strength [11,12]. The challenge lies in reducing an alloy’s elastic modulus without compromising its strength [13,14]. In our previous study [15], we successfully designed a metastable β -type Ti alloy, named Ti-20Zr-40Ta (TZT, at%), based on the Ti-Zr-Ta ternary phase diagram and d-electron orbital theory. By annealing the alloy at 700 °C for 6 h, spinodal decomposition took place, leading to the emergence of two β phases characterized by distinct compositions yet possessing

an identical structure. Remarkably, the as-annealed alloy exhibited enhanced strength attributed to the spinodal strengthening effect while maintaining a negligible increase in its elastic modulus. Therefore, introducing spinodal decomposition into a β -type Ti alloy represents an effective approach to reconcile its high strength and low elastic modulus.

The impact of the wavelength, amplitude, shape, and volume fraction of the decomposition products on the spinodal strengthening effect has been extensively studied and found to be significant [16,17]. Therefore, the aging temperature and duration have a notable impact on the microstructural characteristics and mechanical behavior of Ti alloys undergoing spinodal decomposition. In this study, a Ti-20Zr-40Ta (at%, TZT) alloy was prepared using the arc melting method. The as-cast alloy underwent solid solution treatment at 1100 °C for 0.5 h and was subsequently cold rolled to achieve a thickness reduction of 90%. Subsequently, the as-rolled alloys underwent annealing at temperatures ranging from 550 °C to 850 °C to examine how the microstructure and mechanical properties of the alloy are influenced by variations in annealing temperature and duration.

2. Materials and Methods

2.1. Preparation of TZT Alloy

The Ti-20Zr-40Ta alloy was prepared by vacuum arc melting using pure Ti, Zr, and Ta (99.9% purity, purchased from Beijing Licheng Innovation Metal Materials Technology Co., Ltd., Beijing, China, 99.9% purity) as raw materials. To ensure a uniform composition, the alloy was flipped and repeatedly melted eight times. A button ingot with a diameter of approximately 40 mm and maximum thickness of 15 mm was then cut into a cubic sample measuring 20 × 10 × 10 mm. According to the Ti-Zr-Ta phase diagram, for the Ti-20Zr-40Ta alloy used in the present work, the phase transformation point of a phase to the β phase is about 900 °C. In order to fully consolidate the alloy elements into the titanium matrix, we chose a relatively high temperature, 1100 °C, as the solid solution temperature. So, the as-cast sample was sealed in a vacuum and subjected to solid solution treatment at 1100 °C for 0.5 h in a tubular furnace before being quenched in water. The resulting solid solution-treated sample (referred to as STed sample) underwent cold rolling to form a plate with a thickness reduction rate of about 90%, yielding a final thickness of 1 mm (referred to as CRed sample). Subsequently, the STed sample was sectioned into smaller fragments for subsequent annealing treatment. The CRed samples were hermetically sealed in vacuum silicon tubes and aged at temperatures of 550 °C, 650 °C, 750 °C, and 850 °C for durations of 30 min each (referred to as Aged-550 sample, Aged-650 sample, Aged-750 sample, and Aged-850 sample, respectively). Finally, all samples were quenched in water.

2.2. Characterization of Microstructure and Mechanical Properties

The optical microscope was utilized to observe the microstructures of STed, CRed, and Aged samples. Additionally, X-ray diffraction (XRD, Rigaku D/max2500, Tokyo, Japan) with Cu K α radiation ($\lambda = 1.5406$ nm), operated at 50 kV and 100 mA, respectively, was employed to characterize their phase constitutions. The samples used for optical microscopic (OM, Leica DM2500C, Heidelberg, German) observations and XRD characterizations were cut into dimensions of 5 mm × 5 mm × 1 mm, mounted, ground with SiC sandpapers ranging from 400# to 5000#, and were finally polished to achieve a mirror surface using diamond grinding paste (W 0.5). For the optical microstructure observation, the samples underwent etching in a solution containing 7 vol.% HF. Transmission electron microscope (TEM) observations of the samples were conducted on a JEM-2100 (JEOL Ltd., Tokyo, Japan) operating at an acceleration voltage of 160 KV; TEM samples were prepared using Ar⁺ ion milling. Uniaxial tensile tests were performed on an Instron 5569 universal test machine (Instron, Norwood, MA, USA). Each group of tests was conducted in triplicate, and the resulting data were averaged. The yield strength ($\sigma_{0.2}$) is defined as the stress at which the tensile strain reaches 0.2%. The dimensions of the samples used for the tensile test were measured as follows. The gauge length was 8 mm; the width was 2.5 mm; and the thickness was 1 mm (as schematically shown in Figure 1).

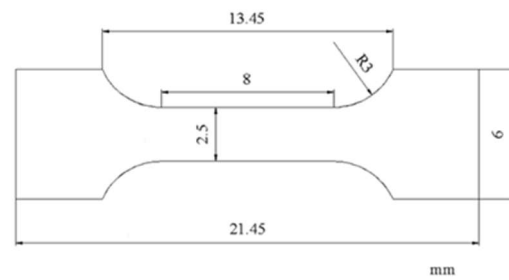


Figure 1. Geometric sketch of the tensile sample.

3. Results and Discussion

3.1. Microstructure

The optical metallurgical images of the STed, CRed, and Aged samples of the TZT alloy are presented in Figure 2. The STed sample exhibited a microstructure characterized by equiaxed grains, with an average size of around 200 μm . After cold rolling, the grains elongated along the rolling direction, resulting in blurred grain boundaries. When the CRed sample was aged at 550 $^{\circ}\text{C}$, its grain morphology did not change significantly, indicating only the occurrence of recovery in the sample aged at 550 $^{\circ}\text{C}$, resulting in a decrease in the density of dislocations in the alloy. As the aging temperature was increased to 650 $^{\circ}\text{C}$, partial recrystallization occurred in the Aged sample, evidenced by the appearance of equiaxed grains in some regions. With the aging temperature further increasing to 750 $^{\circ}\text{C}$, full recrystallization occurred in the Aged sample, in which the elongated grains disappeared and were replaced by the equiaxed grains. The average grain size was measured to be about 150 μm . As the CRed sample was aged at 850 $^{\circ}\text{C}$ for 30 min, its equiaxed grains started to grow, with an average grain size of about 220 μm .

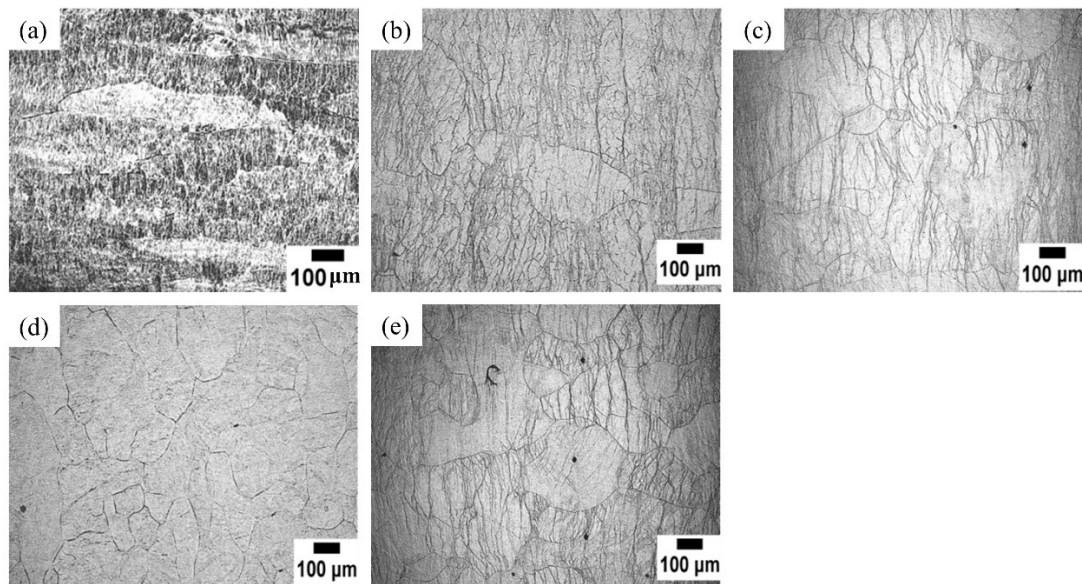


Figure 2. The optical images of the TZT alloys in different states: (a) CRed; (b) Aged-550-30; (c) Aged-650-30; (d) Aged-750-30; (e) Aged-850-30.

The XRD patterns of the STed, CRed, and Aged samples are illustrated in Figure 3. Only diffraction peaks corresponding to the β phase can be observed in the XRD patterns of the STed and CRed samples, indicating that they consist solely of a single β phase due to the addition of β -stabilizing elements Ta and Zr in the Ti alloy (see Figure 3b). In comparison with the STed sample, the diffraction peaks of the β phase in the CRed sample exhibit distinct broadening and slight leftward shifts, suggesting that cold rolling induces lattice

distortion and residual stress within the alloy. Conversely, for samples aged at temperatures ranging from 550 °C to 850 °C, each diffraction peak associated with the β phase split into two peaks on their respective XRD patterns, signifying that spinodal decomposition occurred within these Aged samples. Consequently, this decomposition resulted in two phases (β_1 and β_2) with identical crystal structures (body-centered cubic, BCC structure) but different compositions. A careful examination revealed weak diffraction peaks present on XRD patterns obtained from samples aged at 550 °C, 650 °C, and 750 °C; these can be attributed to the ω phase.

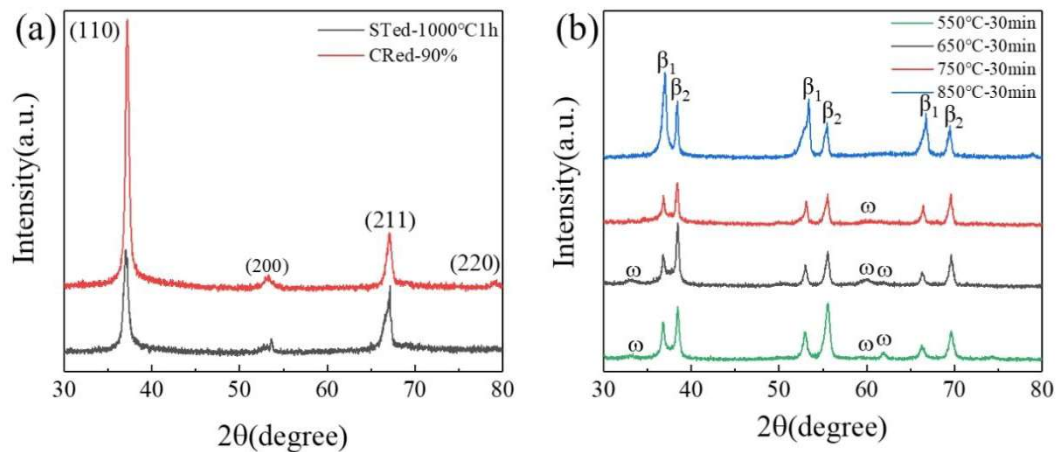


Figure 3. The XRD patterns of the TZT alloys in different states: (a) STed and Cred samples; (b) samples aged at different temperatures.

Close observations were conducted on the samples aged at different temperatures using TEM, and the TEM bright-field images of the aged samples are illustrated in Figure 4. It is evident that nanoscale alternating dark and bright regions are present in all of the aged samples. The SAED pattern reveals the occurrence of diffraction spot splitting in the β phase, supporting the coexistence of two phases (β_1 and β_2). These results indicate that spinodal decomposition occurred during aging treatment, with the morphology of the modulated structure being strongly influenced by aging temperature. For samples aged at 550 °C and 650 °C, oriented strip-shaped spinodal products were observed. As the aging temperature increased to over 750 °C, both precipitate size and shape gradually changed to discrete elliptical or round forms in order to reduce interface energy. Careful observation of the SAED patterns of the samples aged at temperatures in the range of 550 °C revealed that there were some weak diffraction spots (indicated by arrows) superimposed on the diffraction patterns of the β phase. These weak diffraction spots were identified to be from the ω phase, indicating that the ω phase precipitated in the β phase matrix during alloy aging at temperatures ranging from 550 °C to 750 °C. However, when aging temperature reached 850 °C, the ω phase disappeared from the aged sample, which is attributed to its instability at high temperatures over 800 °C [18]. This result suggests that spinodal decomposition decreases β phase stability in the TZT alloy due to formation of Ta-rich and Ta-poor phases; specifically, the Ta-poor phase exhibits low stability for the β phase, resulting in isothermal ω phase formation during aging below 750 °C while becoming unstable above this temperature [19,20], leading to disappearance of the ω phase in samples aged at 850 °C.

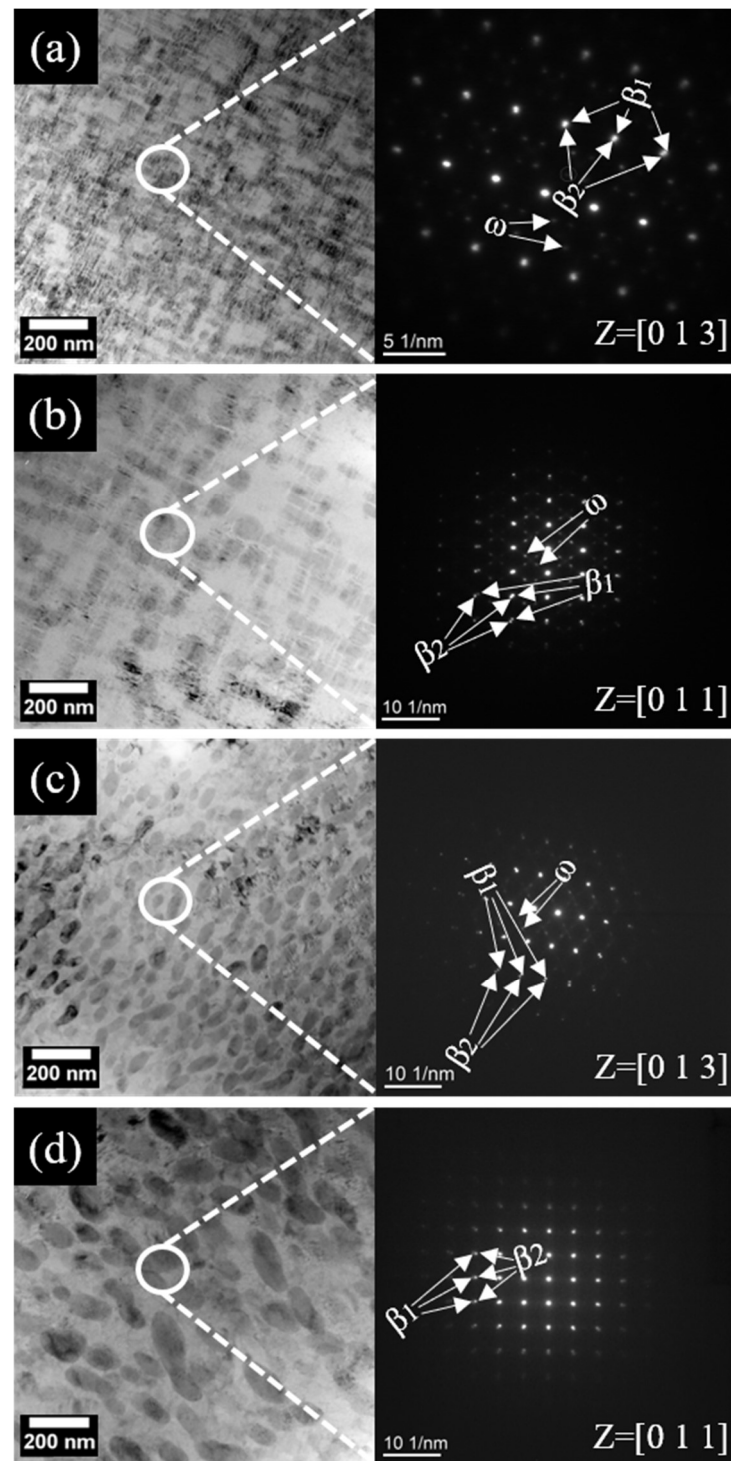


Figure 4. The TEM bright-field images and the corresponding selected area diffraction patterns of the TZT alloys after being aged at different temperatures: (a) 550 °C; (b) 650 °C; (c) 750 °C; (d) 850 °C.

3.2. Mechanical Properties

The stress–strain curves of the STed, Cred, and Aged samples are presented in Figure 5. It is evident that the STed sample exhibits a yield strength of 905 ± 15 MPa with an elongation of 11%. Subsequent cold rolling significantly enhances the alloy's strength while reducing its ductility due to the work hardening effect. Specifically, the CRed sample demonstrates a yield strength of 1460 ± 24 MPa (at 0.2% strain) and an elongation of 3.6%. This enhancement in strength and reduction in ductility can be ascribed to the occurrence

of work-hardening phenomena within the alloy. Aging treatment at 550 °C for 30 min leads to a reduction in strength due to recovery processes while maintaining low ductility. The low ductility of the Aged sample may be associated with the precipitation of the ω phase during aging at both temperatures because the ω phase is with a hexagonal close-packed (HCP) crystal structure, which is very hard and brittle. Notably, stress-curves of samples aged at 650 °C and 750 °C exhibit the presence of two discernible yield points: an initial yield point occurring at a stress level of 310 MPa for the sample aged at 650 °C and at a stress level of 480 MPa for the sample aged at 750 °C. This can be attributed to the β phase transformation into martensite induced by applied stress [21]. The secondary yield point was observed at a stress of 950 ± 16 MPa for the sample aged at 650 °C and 810 ± 18 MPa for the sample aged at 750 °C, indicating plastic deformation of the alloy. This finding implies that spinodal decomposition alters the deformation mechanisms of the alloy by modifying the composition of the β phase.

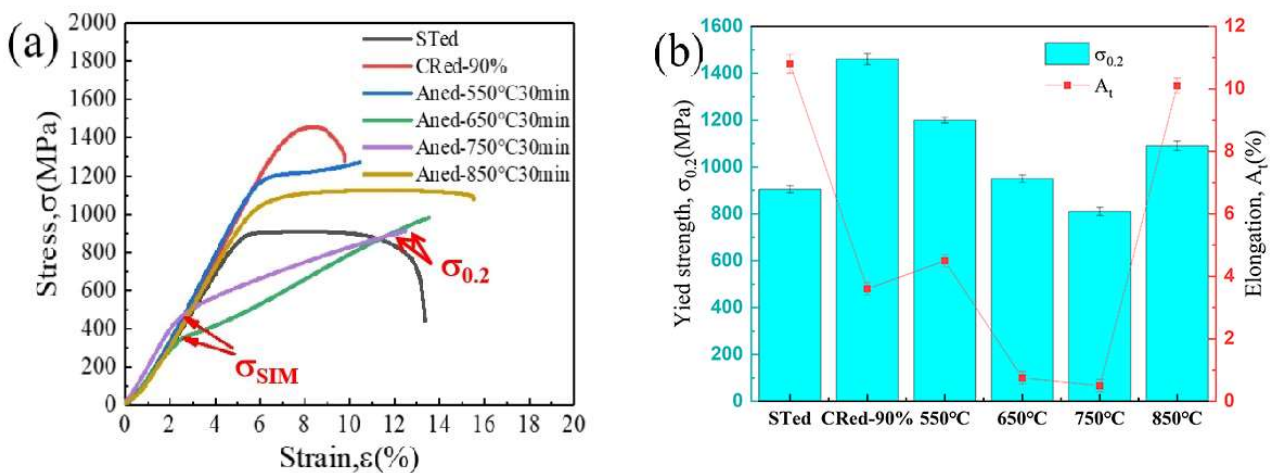


Figure 5. The mechanical properties of the Sted, Cred, and Aged samples of TZT alloy: (a) tensile stress–strain curves; (b) histogram of the yield stress ($\sigma_{0.2}$) and the elongation (A_t).

To validate this, XRD analysis was performed on the sample subjected to tensile testing at 650 °C and 750 °C, as shown in Figure 6. The presence of diffraction peaks corresponding to the β phase indicates the occurrence of stress-induced transformation to martensite (α'') during tensile deformation in the sample aged at 650 °C. Moreover, the samples aged at 650 °C and 750 °C still exhibited very low ductility, and the presence of the ω phases and α'' phases may be responsible for their low ductility. In contrast, for CRed samples aged at 850 °C, the double-yield phenomenon vanished from the stress–strain curves. Although the strength decreased, a significant improvement in plasticity was observed compared to CRed samples due to full recrystallization and the absence of ω phases. Notably, despite recrystallization, samples aged at 850 °C exhibited much higher strength than STed samples. This enhancement can be primarily attributed to a pronounced reinforcing effect resulting from spinodal decomposition and the presence of a modulated structure.

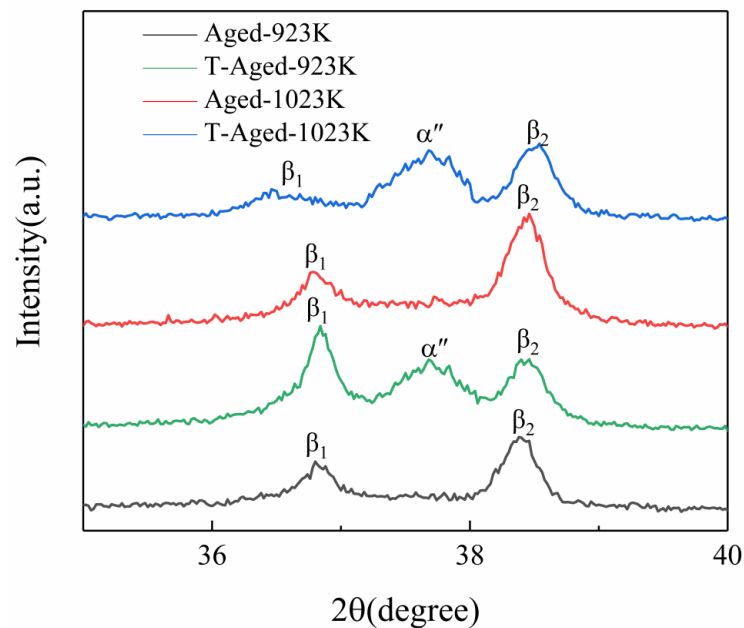


Figure 6. XRD patterns of the samples aged at 650 °C and 750 °C before (Aged sample) and after tensile test (T-Aged sample).

4. Conclusions

(1) The Ti-40Zr-20Ta alloy, primarily composed of the metastable β phase alloy, exhibited a predominant presence of the said phase after undergoing solid solution treatment at 1100 °C and subsequent cold rolling. Subsequently aging the CRed alloy within a temperature range of 550 °C to 850 °C resulted in recovery and recrystallization phenomena, which were dependent on the specific aging temperature. Concurrently, spinodal decomposition occurred during the aging treatment of the CRed alloy, leading to the formation of β_1 and β_2 phases with identical crystal structures but different compositions.

(2) The size and configuration of the spinodal decomposition products exhibited a strong dependence on the temperature of aging and time. As the aging temperature and time increased, both the size of the spinodal decomposition products and their morphology transitioned from oriented strips to distinct elliptical or circular forms. Additionally, when the CRed alloy was aged at temperatures ranging from 550 °C to 750 °C, isothermal ω phases were precipitated in the aged alloys due to a decrease in β phase stability caused by spinodal decomposition. However, when further increasing the aging temperature up to 850 °C, these isothermal ω phases disappeared due to their instability at high temperatures.

(3) The CRed alloy demonstrates high strength and low ductility as a result of work hardening, with yield strength and elongation values of 1460 MPa and 3.6%, respectively. Aging treatment leads to a decrease in the strength of the CRed alloy due to recovery or recrystallization processes, while the temperature at which aging occurs significantly influences its mechanical properties and deformation mechanisms. Tensile tests on as-rolled alloys aged at 650 °C and 750 °C revealed a double-yield phenomenon, indicating martensitic transformation induced by applied stress; however, these alloys exhibited limited ductility due to the presence of ω phases. On the other hand, the alloy aged at 850 °C exhibited comprehensive mechanical properties with a yield strength of 1100 MPa and an elongation of 10%. This improvement in strength may be attributed to the modulated structure introduced by spinodal decomposition.

Author Contributions: X.W.: conceptualization, writing—original draft preparation, and funding acquisition; K.Y.: methodology and data curation; J.C.: investigation and funding acquisition; J.L.: writing—review and editing, supervision, and project administration. All authors have read and agreed to the published version of the manuscript.

Funding: This study was supported by the Doctor Foundation of Guizhou Normal University, the National Natural Science Foundation of China (52271249), and the Key Research and Development Program of Shaanxi (2023-YBGY-488).

Institutional Review Board Statement: Not applicable.

Informed Consent Statement: Not applicable.

Data Availability Statement: The data will be made available upon reasonable request.

Conflicts of Interest: The authors declare no conflicts of interest.

References

1. Cma, B.; Lac, A.; Lhc, A.; Hm, C. Microstructure and mechanical properties of selective laser melted Ti-3Al-8V-6Cr-4Zr-4Mo compared to Ti-6Al-4V. *Mater. Sci. Eng. A* **2019**, *747*, 225–231. [[CrossRef](#)]
2. Reilly, D.T.; Burstein, A.H.; Frankel, V.H. The elastic modulus for bone. *J. Biomech.* **1974**, *7*, 271–275. [[CrossRef](#)] [[PubMed](#)]
3. Zhang, L.; Chen, L. A Review on Biomedical Titanium Alloys: Recent Progress and Prospect. *Adv. Eng. Mater.* **2019**, *21*, 1801215. [[CrossRef](#)]
4. Ren, D.C.; Zhang, H.B.; Liu, Y.J.; Li, S.J.; Zhang, L.C. Microstructure and properties of equiatomic Ti-Ni alloy fabricated by selective laser melting. *Mater. Sci. Eng. A* **2019**, *771*, 138586. [[CrossRef](#)]
5. Abdel-Hady, M.; Hinoshita, K.; Morinaga, M. General approach to phase stability and elastic properties of β -type Ti-alloys using electronic parameters. *Scr. Mater.* **2006**, *55*, 477–480. [[CrossRef](#)]
6. Kuroda, D.; Niinomi, M.; Morinaga, M.; Kato, Y.; Yashiro, T. Design and mechanical properties of new β type titanium alloys for implant materials. *Mater. Sci. Eng. A* **1998**, *243*, 244–249. [[CrossRef](#)]
7. Zhao, Z.; Wang, C.; Yu, Q.; Song, L.; Yang, G.; Zhang, J. New β -type Ti-Zr-V-Nb alloys used for laser-based direct energy deposition: Design, microstructure, and properties. *Mater. Charact.* **2022**, *189*, 111917. [[CrossRef](#)]
8. Hsu, H.-C.; Wong, K.-K.; Wu, S.-C.; Chen, Y.-X.; Ho, W.-F. Metastable dual-phase Ti-Nb-Sn-Zr and Ti-Nb-Sn-Fe alloys with high strength-to-modulus ratio. *Mater. Today Commun.* **2022**, *30*, 103168. [[CrossRef](#)]
9. Hagihara, K.; Nakano, T.; Maki, H.; Umakoshi, Y.; Niinomi, M. Isotropic plasticity of β -type Ti-29Nb-13Ta-4.6Zr alloy single crystals for the development of single crystalline β -Ti implants. *Sci. Rep.* **2016**, *6*, 29779. [[CrossRef](#)]
10. Yang, Y.; Castany, P.; Cornen, M.; Prima, F.; Li, S.J.; Hao, Y.L.; Gloriant, T. Characterization of the martensitic transformation in the superelastic Ti-24Nb-4Zr-8Sn alloy by in situ synchrotron X-ray diffraction and dynamic mechanical analysis. *Acta Mater.* **2015**, *88*, 25–33. [[CrossRef](#)]
11. Xiang, T.; Du, P.; Cai, Z.; Li, K.; Bao, W.; Yang, X.; Xie, G. Phase-tunable equiatomic and non-equiatomic Ti-Zr-Nb-Ta high-entropy alloys with ultrahigh strength for metallic biomaterials. *J. Mater. Sci. Technol.* **2022**, *117*, 196–206. [[CrossRef](#)]
12. Wang, W.; Yang, K.; Wang, Q.; Dai, P.; Fang, H.; Wu, F.; Guo, Q.; Liaw, P.K.; Hua, N. Novel Ti-Zr-Hf-Nb-Fe refractory high-entropy alloys for potential biomedical applications. *J. Alloys Compd.* **2022**, *906*, 164383. [[CrossRef](#)]
13. Hua, N.; Wang, W.; Wang, Q.; Ye, Y.; Lin, S.; Zhang, L.; Guo, Q.; Brechtel, J.; Liaw, P.K. Mechanical, corrosion, and wear properties of biomedical Ti-Zr-Nb-Ta-Mo high entropy alloys. *J. Alloys Compd.* **2021**, *861*, 157997. [[CrossRef](#)]
14. Xiao, X.; Yang, K.; Lei, S.; Zhang, D.; Guo, L.; Dai, Y.; Lin, J. A β -type Titanium alloy with high strength and low elastic modulus achieved by spinodal decomposition. *J. Alloys Compd.* **2023**, *963*, 171270. [[CrossRef](#)]
15. Wu, R.; Yi, Q.; Lei, S.; Dai, Y.; Lin, J. Design of Ti-Zr-Ta Alloys with Low Elastic Modulus Reinforced by Spinodal Decomposition. *Coatings* **2022**, *12*, 756. [[CrossRef](#)]
16. Langer, J.S. Theory of spinodal decomposition in alloys. *Ann. Phys.* **1971**, *65*, 53–86. [[CrossRef](#)]
17. Yang, K.; Wang, Y.; Tang, J.; Wang, Z.; Zhang, D.; Dai, Y.; Lin, J. Phase Field Study on the Spinodal Decomposition of β Phase in Zr-Nb-Ti Alloys. *Materials* **2023**, *16*, 2969. [[CrossRef](#)] [[PubMed](#)]
18. Bailor, J.; Li, T.; Prima, F.; Boehlert, C.J.; Devaraj, A. A review of the metastable omega phase in beta titanium alloys: The phase transformation mechanisms and its effect on mechanical properties. *Int. Mater. Rev.* **2023**, *68*, 26–45. [[CrossRef](#)]
19. Sikka, S.K.; Vohra, Y.K.; Chidambaram, R. Omega phase in materials. *Prog. Mater. Sci.* **1982**, *27*, 245–310. [[CrossRef](#)]
20. Weiss, I.; Semiatin, S.L. Thermomechanical processing of alpha titanium alloys—An overview. *Mater. Sci. Eng. A* **1999**, *263*, 243–256. [[CrossRef](#)]
21. Biesiekierski, A.; Ping, D.; Li, Y.; Lin, J.; Munir, K.S.; Yamabe-Mitarai, Y.; Wen, C. Extraordinary high strength Ti-Zr-Ta alloys through nanoscaled, dual-cubic spinodal reinforcement. *Acta Biomater.* **2017**, *53*, 549–558. [[CrossRef](#)] [[PubMed](#)]

Disclaimer/Publisher’s Note: The statements, opinions and data contained in all publications are solely those of the individual author(s) and contributor(s) and not of MDPI and/or the editor(s). MDPI and/or the editor(s) disclaim responsibility for any injury to people or property resulting from any ideas, methods, instructions or products referred to in the content.